Bottomonium and Drell–Yan production in $p–A$ collisions at 450 GeV

NA50 Collaboration

B. Alessandro [j], C. Alexa [c], R. Arnaldi [j], M. Atayan [l], S. Beolè [j], V. Boldea [c], P. Bordalo [f,1], G. Borges [f], J. Castor [b], B. Chaurand [i], B. Cheynis [k], E. Chiavassa [j], C. Cicalò [d], M.P. Comets [h], S. Constantinescu [c], P. Cortese [a], A. De Falco [d], N. De Marco [j], G. Dellacasa [a], A. Devaux [b], S. Dita [c], J. Fargeix [b], P. Force [b], M. Gallio [j], C. Gerschel [h], P. Giubellino [j], M.B. Golubeva [g], A. Grigoryan [l], J.Y. Grossiord [k], F.F. Guber [g], A. Guichard [k], H. Gulkanyan [l], M. Idzik [j,2], D. Jouan [h], T.L. Karavicheva [g], L. Kluberg [i], A.B. Kurepin [g], Y. Le Bornec [h], C. Lourenço [e], M. Mac Cormick [h], A. Marzari-Chiesa [j], M. Masera [j], A. Masoni [d], M. Monteno [j], A. Musso [j], P. Petiau [i], A. Piccotti [j], J.R. Pizzi [k], F. Prino [j], G. Puddu [d], C. Quintans [f], L. Ramello [a], S. Ramos [f,1], L. Riccati [j], H. Santos [f], P. Saturnini [b], E. Scomparin [j,*], S. Serci [d], R. Shahoyan [f,3], M. Sitta [a], P. Sonderegger [e,1], X. Tarrago [h], N.S. Topilskaya [g], G.L. Usai [d], E. Vercellin [j], N. Willis [h]

[a] Università del Piemonte Orientale, Alessandria and INFN, Torino, Italy
[b] LPC, Université Blaise Pascal and CNRS-IN2P3, Aubière, France
[c] IFA, Bucharest, Romania
[d] Università di Cagliari/INFN, Cagliari, Italy
[e] CERN, Geneva, Switzerland
[f] LIP, Lisbon, Portugal
[g] INR, Moscow, Russia
[h] IPN, Université de Paris-Sud and CNRS-IN2P3, Orsay, France
[i] LLR, Ecole Polytechnique and CNRS-IN2P3, Palaiseau, France
[j] Università di Torino/INFN, Torino, Italy
[k] IPN, Université Claude Bernard Lyon-I and CNRS-IN2P3, Villeurbanne, France
[l] YerPhI, Yerevan, Armenia

Received 20 December 2005; accepted 2 March 2006

Available online 10 March 2006

Editor: W.-D. Schlatter

Abstract

The NA50 Collaboration has measured heavy-quarkonium production in $p–A$ collisions at 450 GeV incident energy ($\sqrt{s} = 29.1$ GeV). We report here results on the production of the Υ states and of high-mass Drell–Yan muon pairs ($m_{\mu\mu} > 6$ GeV/c^2). The cross-section at midrapidity and the A-dependence of the measured yields are determined and compared with the results of other fixed-target experiments and with the available theoretical estimates. Finally, we also address some issues concerning the transverse momentum distributions of the measured dimuons.
© 2006 Elsevier B.V. Open access under CC BY license.

---

* Corresponding author.
  E-mail address: scomparin@to.infn.it (E. Scomparin).
[1] Also at 1ST, Universidade Técnica de Lisboa, Lisbon, Portugal.
[2] Also at Faculty of Physics and Nuclear Techniques, AGH University of Science and Technology, Cracow, Poland.
[3] On leave of absence of YerPhI, Yerevan, Armenia.

1. Introduction

The study of heavy quarkonium states is very important for our understanding of the physics of strong interactions and represents today one of the most challenging fields of application of QCD [1]. By studying quarkonium production in p–A collisions at fixed-target energies, various aspects of the theory of strong interactions can be addressed. In particular, such data can be used to constrain theoretical approaches used for the calculation of the production cross-section in nucleon–nucleon interactions, such as the color-evaporation model (CEM) [2] or the nonrelativistic QCD formulation (NRQCD) [3]. Furthermore, by comparing the production data on various nuclear targets, the details of the color neutralization process of the $q\bar{q}$ pair can be investigated [4–6]. Finally, p–A data are an essential reference for the study of the anomalous suppression of quarkonia production predicted to occur in ultrarelativistic heavy-ion collisions [7–9].

To investigate these topics, the NA50 Collaboration performed a systematic study of quarkonium production on several nuclear targets with proton beams at 450 GeV/c incident momentum. Results on the charmonium states J/ψ and ψ', detected through their decay into two muons, have already been published [10,11]. Thanks to the large integrated luminosity ($\sim$10 pb^{-1} for each target), the dimuon mass spectrum also shows a signal corresponding to the sum of the $\Upsilon(1S)$, $\Upsilon(2S)$ and $\Upsilon(3S)$ states (simply denoted as Υ in the following).

Various results on Υ production in proton-induced collisions exist at fixed target and at ISR energies [12–25], but they are usually less precise than the corresponding charmonium results. Up to now, no data are available at 450 GeV ($\sqrt{s} = 29.1$ GeV), and the A-dependence of the production cross-section has only been studied by the E772 experiment [22], at a higher incident energy.

In this Letter we show results on the production of the Υ in proton-induced collisions on five nuclear targets (Be, Al, Cu, Ag, W). After applying the appropriate cuts, the total number of Υ meson events is of the order of 300. We compute, for the various targets, the cross-sections around midrapidity for the Υ, as well as for Drell–Yan muon pairs with invariant mass larger than 6 GeV/c^2. We parametrize these cross-sections with the usual relation $\sigma_A = \sigma_N A^\alpha$, and determine the values α_Υ and α_{DY}. We also determine the A-dependence of the ratio $B_{\mu\mu}\sigma_\Upsilon/\sigma_{DY}$, a quantity less affected by systematical effects. Then, by combining the results for the different target nuclei, we obtain $B_{\mu\mu} \, d\sigma/dy_{cm}|_{y_{cm}=0}$, a quantity that can be compared with the results of other experiments and with theoretical calculations. Finally, the dependences of $\langle p_T \rangle$ and $\langle p_T^2 \rangle$ on A and $\sqrt{s}$ are discussed.

2. Experimental setup and data analysis

The setup of the NA50 experiment has been described in detail in various publications [26]. It is based on a muon spectrometer composed of a 5 meter long hadron absorber, an air-core toroidal magnet and various sets of MWPCs and scintillator hodoscopes. The luminosity measurement is achieved by means

Table 1
Quantities used in the cross-section calculation

	N_Υ	N_{DY} ($m_{\mu\mu} > 6$ GeV/c^2)	$\mathcal{L}$ (pb^{-1})	$\epsilon_{\mu\mu}$	ϵ_{trig}
p–Be	26 ± 9	485 ± 23	52.2	0.86	0.87
p–Al	82 ± 13	901 ± 31	30.2	0.87	0.88
p–Cu	67 ± 13	1110 ± 34	17.1	0.84	0.89
p–Ag	65 ± 14	1243 ± 37	9.9	0.86	0.89
p–W	63 ± 12	820 ± 30	4.7	0.84	0.87

of three argon ionization chambers placed along the beam path. They have been calibrated at low beam intensity and their linearity has been checked up to 10^{10} p/s [27]. The intensity of the 450 GeV proton beam delivered by the SPS was about 3×10^9 p/burst, with a 2.3 s spill. The thickness of the targets ranged from 30 to 50% of an interaction length. In these conditions, the dimuon trigger rate was $\sim 10^3$/burst, with a dead time smaller than 5%. The efficiency ϵ_{trig} of the dimuon trigger system has been measured during data taking, using dedicated hardware, and ranges from 87 to 89% (see Table 1). About 50% of the triggered events contain a dimuon, which is reconstructed with the improved version of the reconstruction algorithm described in Refs. [11,28]. The dimuon reconstruction efficiency, $\epsilon_{\mu\mu}$, is dominated by the efficiency of the MWPCs and is determined by the reconstruction program. Its precise value, used as input to obtain the cross-sections, depends on the data taking conditions and ranges from 84 to 87% (see Table 1). Various quality cuts are applied, to remove parasitic off-target events. Furthermore, in order to discard dimuons produced at the edge of the acceptance of the spectrometer, the kinematical domain of the analysis is restricted to $-0.5 < y_{cm} < 0.5$ in rapidity and to $-0.5 < \cos\theta_{CS} < 0.5$ in the Collins–Soper polar angle of the muons [29]. We are finally left with about 1000 high mass events ($m_{\mu\mu} > 6$ GeV/c^2) for each target.

Fig. 1 shows the five invariant mass spectra, in the region $m_{\mu\mu} > 6$ GeV/c^2. The Υ signal can be clearly seen on top of a continuum due to the Drell–Yan process. In this mass region the combinatorial background due to π and K decays, usually calculated through the measured like-sign dimuon sample, turns out to be negligible. Muon pairs originating from Drell–Yan and from the Υ resonances are estimated by means of a fit to the invariant mass spectrum. The mass shapes for the various processes have been calculated through a Monte Carlo simulation. The Drell–Yan events have been generated using a LO QCD calculation, with the GRV94LO set of parton distribution functions [30]; the p_T distributions have been tuned directly on the data (see Section 3 for details) and, in the considered mass range, they do not significantly depend on the dimuon mass. The bottomonium states have been generated at their nominal PDG mass [31]. Due to the invariant mass resolution of the spectrometer, of the order of 0.4 GeV/c^2 for dimuons with $m_{\mu\mu} \sim 10$ GeV/c^2, the various Υ states cannot be resolved. We have, therefore, relied on previous measurements to fix the relative contributions of the three states visible in the dimuon channel. We have used the values $\Upsilon(2S)/\Upsilon(1S) = 0.32$ and $\Upsilon(3S)/\Upsilon(1S) = 0.13$, as measured
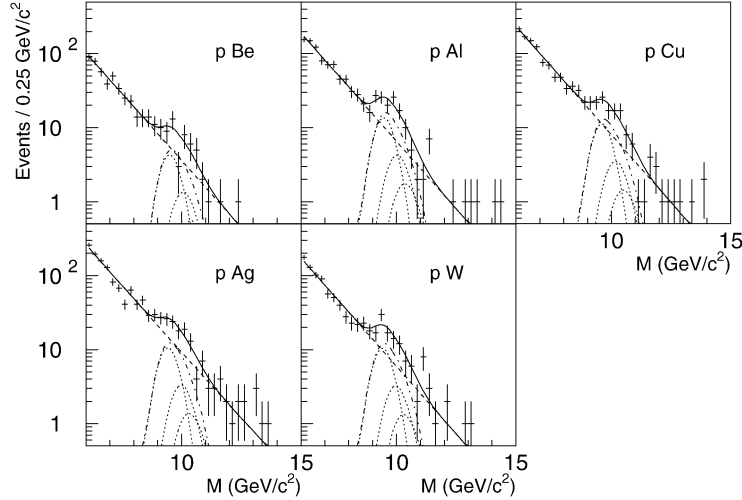
Fig. 1. The five p–A opposite-sign muon pair mass spectra, in the mass range $m_{\mu\mu} > 6$ GeV/c^2. The solid line is the result of the fit with the function described in Eq. (2). The dashed line represents the Drell–Yan process, the dotted lines the contributions of the various bottomonium states, the dot-dashed line the sum of the three Υ states.

in p–A collisions at 400 GeV [14], i.e., close to our energy. The results of Ref. [14] are anyway compatible with a high statistics measurement performed at higher energy [21]. For the bottomonium p_T distribution, we have adopted the functional form

$$\mathrm{d}\sigma/\mathrm{d}p_T \propto p_T / \left[1 + (p_T/p_0)^2 \right]^6, \qquad (1)$$

used in Ref. [21]. The p_0 parameter has been fitted on the measured p_T distributions (see Section 3).

For the rapidity, due to the narrow coverage of the set-up and to the relatively small statistics, our data do not allow a precise determination of the Υ y-distribution. As a first guess, we have used in the acceptance calculation a Gaussian distribution, centered at $y_{cm} = 0$, with $\sigma_y = 0.37 \pm 0.01$. This value comes from a fit to the x_F distribution for Υ production at 400 GeV ($\sigma_y = 0.35 \pm 0.01$) [14,19]. The obtained value has then been logarithmically scaled to our incident energy. In Section 3 we will investigate in more detail the influence of the rapidity shape on our Υ results. Finally, the $\cos\theta_{CS}$ distributions for the Υ states have been generated according to the recent results of the E866 Collaboration [24], which found a negligible polarization for the Υ(1S) around midrapidity and a large transverse polarization for the Υ(2S) and Υ(3S) states. The generated Drell–Yan and Υ events have then been tracked through the apparatus and the accepted events have been reconstructed using the procedure applied to the experimental data. With the choice of the generation parameters described above, the acceptances for the various dimuon sources turn out to be $A_{DY} = 21\%$ ($m_{\mu\mu} > 6$ GeV/c^2), $A_{\Upsilon(1S)} = 25\%$, $A_{\Upsilon(2S)} = 25\%$, $A_{\Upsilon(3S)} = 26\%$. These acceptances refer to the phase space domain $\mathcal{D}$ defined by the cuts $-0.5 < y_{cm} < 0.5$ and $-0.5 < \cos\theta_{CS} < 0.5$. The error on the acceptances due to the uncertainty on the rapidity distribution is less than 1%.

Having calculated the shapes of the expected contributions, we fit each of the five invariant mass spectra with the function

$$\frac{\mathrm{d}N^{+-}}{\mathrm{d}M} = N^{\mathrm{DY}} \frac{\mathrm{d}N^{\mathrm{DY}}}{\mathrm{d}M}$$

$$+ N^{\Upsilon} \left(\frac{\mathrm{d}N^{\Upsilon(1S)}}{\mathrm{d}M} + 0.32 \cdot \frac{A_{\Upsilon(2S)}}{A_{\Upsilon(1S)}} \frac{\mathrm{d}N^{\Upsilon(2S)}}{\mathrm{d}M} \right.$$

$$\left. + 0.13 \cdot \frac{A_{\Upsilon(3S)}}{A_{\Upsilon(1S)}} \frac{\mathrm{d}N^{\Upsilon(3S)}}{\mathrm{d}M} \right), \qquad (2)$$

where N^{DY} and N^{Υ} are free parameters in the fit. To compensate for possible approximations in the description of the setup and in the mapping of the magnetic field we leave the position of the Υ(1S) peak as a further free parameter in the fit. The mass differences $m_{\Upsilon(2S)} - m_{\Upsilon(1S)}$ and $m_{\Upsilon(3S)} - m_{\Upsilon(1S)}$ are anyway kept fixed to their PDG values [31]. We find that the shift from the nominal mass of the bottomonium states does not exceed 1% and has negligible consequences ($< 1\%$) on the estimated Υ yield.

The choice of the fit region is dictated by the request of having a negligible contribution of the charmonia states. To satisfy this request, one could start the fit at mass values around 4.5 GeV/c^2. However, due to the steep slope of the Drell–Yan mass distributions, the use of a large fit window results in a loss of weight of the low-statistics Υ region. In this way, small inaccuracies in the Monte Carlo description of the Drell–Yan might influence the estimate of the Υ yield. Pushing down to 4.5 GeV/c^2 the starting point of the fit, the change in the calculated number of Drell–Yan and Υ events is only 10% on average, but the χ^2 of the fits are worsened by about 50%. Therefore, we have started our fits at $m_{\mu\mu} = 6$ GeV/c^2. In this way, as can be seen in Fig. 1, the measured invariant mass spectra are well reproduced, with values of χ^2/ndf ranging from 0.9 to 1.5. The number of Υ mesons and the number of high mass Drell–Yan pairs are reported in Table 1.

Finally, the Drell–Yan and Υ cross-sections, in the kinematical domain $\mathcal{D}$ defined above, have been calculated through the

formula

$$\sigma_{\mathcal{D}}^i = \frac{N_i}{A_i} \cdot \frac{1}{\mathcal{L} \cdot \epsilon_{\mu\mu} \cdot \epsilon_{\text{trig}}}, \tag{3}$$

where N_i is the number of detected events for each process i, $\mathcal{L}$ is the luminosity, corrected for dead time, A_i is the acceptance, $\epsilon_{\mu\mu}$ is the dimuon reconstruction efficiency and ϵ_{trig} is the efficiency of the dimuon trigger. For the Υ, we calculate the cross-section integrated over the $\Upsilon(1S)$, $\Upsilon(2S)$ and $\Upsilon(3S)$ states. The values of the various quantities relevant for the determination of the cross-section are summarized in Table 1.

3. Results

In Fig. 2 we show, as a function of the mass number A, the Drell–Yan cross-sections divided by A. The points refer to the kinematical domain $\mathcal{D}$, and to the mass range $m_{\mu\mu} > 6$ GeV/c^2. The error bars shown in Fig. 2 represent the quadratic combination of statistical and systematical errors. The systematical errors on the cross-section measurements are due to the errors on the determination of the incident proton flux and on the evaluation of ϵ_{trig} and $\epsilon_{\mu\mu}$ [11]. They range from 3.4 to 3.7% and are comparable to the statistical errors. The quantity σ_{DY}/A corresponds to the cross-section per nucleon–nucleon collision. In absence of final state interactions, and if nuclear effects on the PDFs are negligible, a flat behaviour is expected. By fitting the points with the function

$$\sigma_{\text{DY}}^{pA} = \sigma_{\text{DY}}^{pp} \cdot A^{\alpha\text{DY}} \tag{4}$$

we get $\alpha_{\text{DY}} = 0.98 \pm 0.02$ ($\chi^2/\text{ndf} = 3.1$), a value compatible with 1. Alternatively, imposing $\alpha = 1$ results in the line shown in Fig. 2, with $\chi^2/\text{ndf} = 2.5$. This result is in fair agreement with previous observations by NA50 in a lower mass range
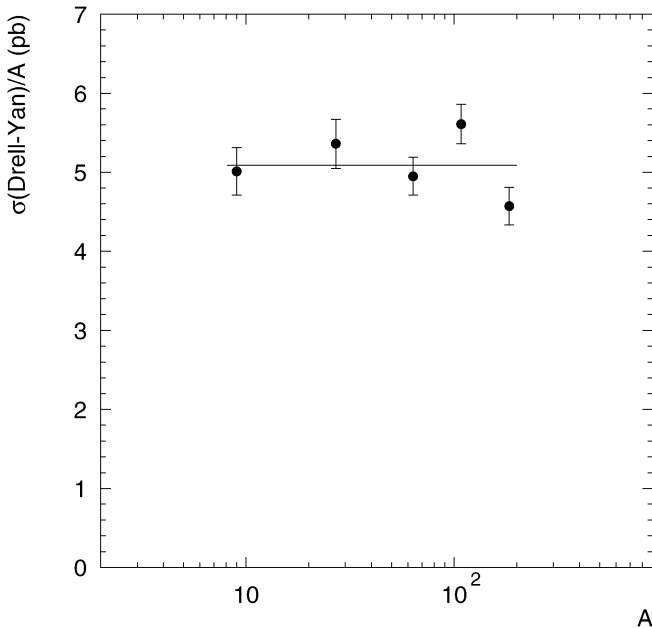

Fig. 2. The Drell–Yan cross-section, relative to the mass region $m_{\mu\mu} > 6$ GeV/c^2, divided by the mass number A. The line represents the result of a fit to the points, according to the function $\sigma_{\text{DY}}^{pA} = \sigma_{\text{DY}}^{pp} \cdot A$.

[10,11], showing that the Drell–Yan cross-section scales with the number of nucleon–nucleon collisions.

Fig. 3 shows the A-dependence of bottomonium production, through the ratio $B_{\mu\mu}\sigma_\Upsilon/\sigma_{\text{DY}}$, where $B_{\mu\mu}\sigma_\Upsilon$ refers to the sum of the 1S, 2S and 3S states, weighted by their branching ratio into two muons. The quantity $B_{\mu\mu}\sigma_\Upsilon/\sigma_{\text{DY}}$ is proportional to the bottomonium cross-section per nucleon–nucleon collision. Being the ratio of two measured cross-sections it is less affected by systematical errors. In the same figure we show the quantity $B_{\mu\mu}\sigma_\Upsilon/A$ as a function of A. Again, the plotted errors represent a quadratic combination of statistical and systematical errors. The values of the various cross-sections and of their ratios are shown in Table 2.

The fits of the two sets of points to the usual A^α parameterization give $\alpha_{\Upsilon/\text{DY}} = 0.98 \pm 0.10$ ($\chi^2/\text{ndf} = 1.7$) and $\alpha_\Upsilon = 0.98 \pm 0.10$ ($\chi^2/\text{ndf} = 1.7$). Within the rather large statistical errors, our result indicates that the Υ is not strongly absorbed in the nuclear medium. In particular, by imposing $\alpha = 1$ (solid lines in Fig. 3), we can describe the data with $\chi^2/\text{ndf} = 1.3$ for Υ/DY and for σ_Υ. We find that our result is compatible with the only other direct determination of the A-dependence of Υ production, carried out by E772 [22] at 800 GeV incident energy.

Assuming $\alpha_\Upsilon = 1$, as suggested by our data, we averaged the results on the various targets and obtained for the Υ cross-section per nucleon–nucleon collision the value $B_{\mu\mu}\sigma_\Upsilon = 0.27 \pm 0.03$ pb/nucleon. As a further check of possible systematic effects, we also obtained the same quantity through the analysis of a different data sample, taken by NA50 [10] at a beam intensity about one order of magnitude lower and containing 72 ± 12 Υ events. We get $B_{\mu\mu}\sigma_\Upsilon = 0.32 \pm 0.06$ pb/nucleon. The two values of σ_Υ agree within errors, indicating that the high-luminosity data analyzed in this Letter have been properly corrected for the various efficiency factors, whose evaluation is more delicate at high beam intensities. For completeness, we show in Fig. 4, as a function of A, $B_{\mu\mu}\sigma_\Upsilon/\sigma_{\text{DY}}$ and $B_{\mu\mu}\sigma_\Upsilon$ for the low beam intensity sample. Performing a simultaneous fit of the data sets of Figs. 3 and 4, we get $\alpha_{\Upsilon/\text{DY}} = 0.98 \pm 0.09$ ($\chi^2/\text{ndf} = 0.9$) and $\alpha_\Upsilon = 0.98 \pm 0.08$ ($\chi^2/\text{ndf} = 0.8$).

The Υ cross-section per nucleon–nucleon collision can be compared with previous measurements performed by various fixed-target experiments. However, past experiments usually quote the quantity $B_{\mu\mu}\,d\sigma/dy_{\text{cm}}|_{y_{\text{cm}}=0}$, and assumptions different from ours have sometimes been adopted in the cross-section calculations. In particular, past experiments evaluated their acceptances assuming an unpolarized production of the Υ states. Furthermore, in some cases they applied a correction to take into account the Fermi-motion of the target nucleons. In order to properly compare our results with the ones available in the literature, we have first recalculated our acceptances assuming no polarization for all the three bottomonium states. With respect to the results shown in Figs. 3 and 4 we get a 1.5% decrease in the value of the cross-section. The influence of Fermi motion has been taken into account by applying to our results (and to the ones available in the literature not yet corrected) the correction proposed in Ref. [13]. At our center of
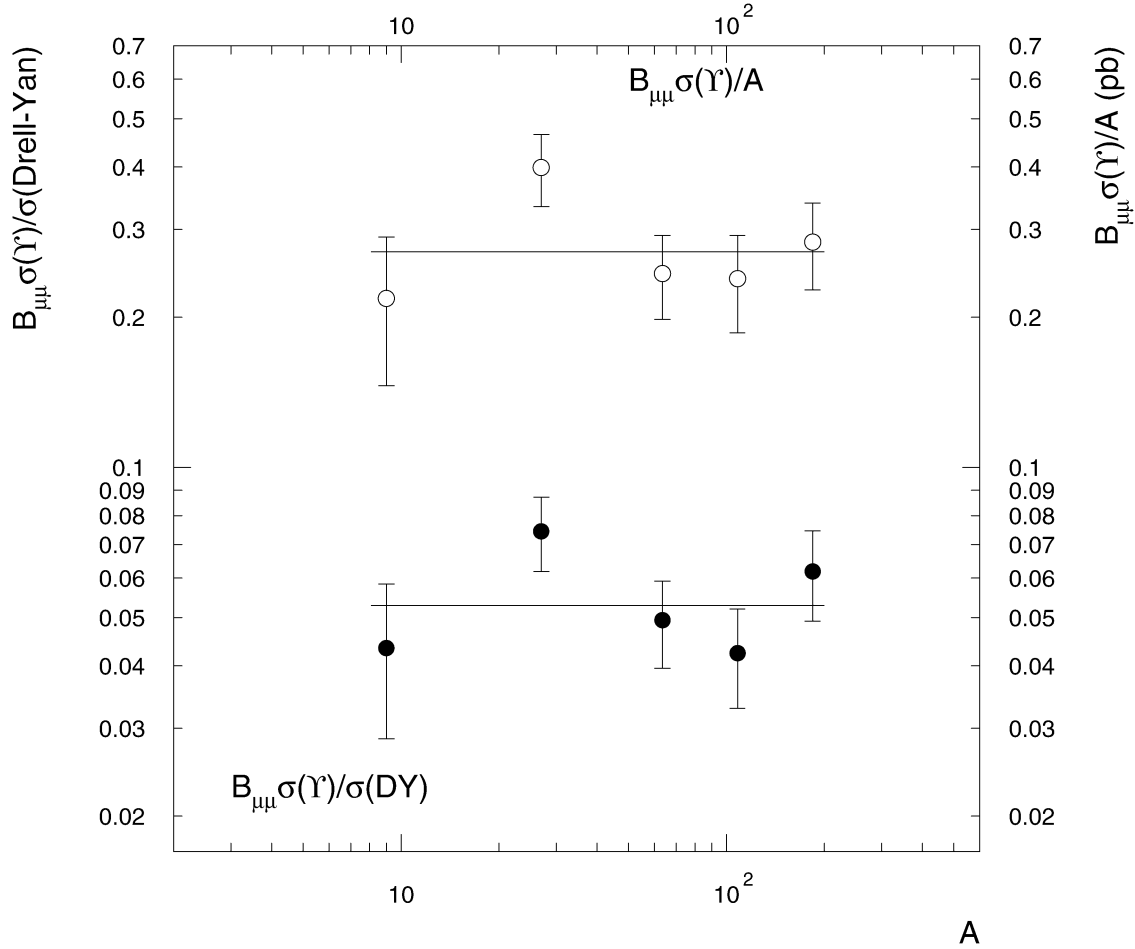
Fig. 3. The ratio $B_{\mu\mu}\sigma_\Upsilon/\sigma_{DY}$ (closed circles) and the cross-section per nucleon. $B_{\mu\mu}\sigma_\Upsilon/A$ (open circles), as a function of A.

Table 2
Drell–Yan (for the mass region $m_{\mu\mu} > 6$ GeV/c^2) and bottomonium cross-sections, and their ratio. The first error is statistical, the second systematical. The quoted systematical errors cancel out in the ratio $B_{\mu\mu}\sigma_\Upsilon/\sigma_{DY}$

	σ_{DY}/A (pb)	$B_{\mu\mu}\sigma_\Upsilon/A$ (pb)	$B_{\mu\mu}\sigma_\Upsilon/\sigma_{DY}$
p–Be	$5.01 \pm 0.24 \pm 0.18$	$0.218 \pm 0.072 \pm 0.008$	0.044 ± 0.015
p–Al	$5.36 \pm 0.19 \pm 0.25$	$0.399 \pm 0.063 \pm 0.019$	0.075 ± 0.012
p–Cu	$4.95 \pm 0.15 \pm 0.19$	$0.245 \pm 0.046 \pm 0.009$	0.049 ± 0.010
p–Ag	$5.61 \pm 0.17 \pm 0.19$	$0.239 \pm 0.052 \pm 0.008$	0.043 ± 0.009
p–W	$4.57 \pm 0.17 \pm 0.17$	$0.283 \pm 0.055 \pm 0.010$	0.062 ± 0.013

mass energy, $\sqrt{s} = 29.1$ GeV, the factor to apply to the results is 0.897.

Concerning the A-dependence, all the other experiments also assumed $\alpha = 1$.

A further element in the calculation of the midrapidity cross-section is the rapidity shape assumed for the Υ production. In fact, due to the limited y-coverage of the NA50 setup, our result may be sensitive to the chosen rapidity shape. We find that the rapidity distribution of the Υ mesons in our sample is compatible with a Gaussian having $\sigma_y^\Upsilon > 0.30$ (95% c.l.). Indeed, it is even compatible with a flat y-distribution. The value for $B_{\mu\mu}\,d\sigma/dy_{cm}|_{y_{cm}=0}$ varies by $^{+7\%}_{-15\%}$ in these two extreme cases, and we consider this uncertainty as a contribution to the sys-

tematical error in the determination of the mid-rapidity cross-section.

The obtained value is $B_{\mu\mu}\,d\sigma/dy|_{y_{cm}=0} = 0.65 \pm 0.05^{+0.04}_{-0.10}$ pb/nucleon, where the quoted asymmetric error is due to the uncertainty on the Υ rapidity distribution as derived from our data. In Fig. 5 we present the $\sqrt{s}$-dependence of the Υ cross-section per nucleon–nucleon collision. The NA50 point is in good agreement with the available systematics. We also plot in Fig. 5 the results of a NLO calculation based on the color evaporation model (CEM) [33]. The curves are obtained by fitting the data with various combinations of the CEM parameters, namely the mass of the b-quark, the renormalization/factorization scale and the choice of the PDF set. It can be seen that the $\sqrt{s}$ dependence of the Υ cross-section is well reproduced. For the other model commonly used in the study of heavy quarkonia cross-sections, NRQCD, no up-to-date calculation exists in the literature. The only available prediction [34] gives a value of the order of 50 pb/nucleon for the total Υ cross-section at $\sqrt{s} = 29.1$ GeV. By integrating our differential cross-section over y and $\cos\theta_{CS}$, and correcting for the branching ratios, we get $\sigma_{tot}^\Upsilon = 29 \pm 2^{+31}_{-4}$ pb/nucleon. The asymmetric systematic error is dominated by the uncertainty in the rapidity distribution derived from our data. If we rely on the data from previous experiments for the determination of σ_y^Υ the systematic error is reduced to ± 2 pb/nucleon.
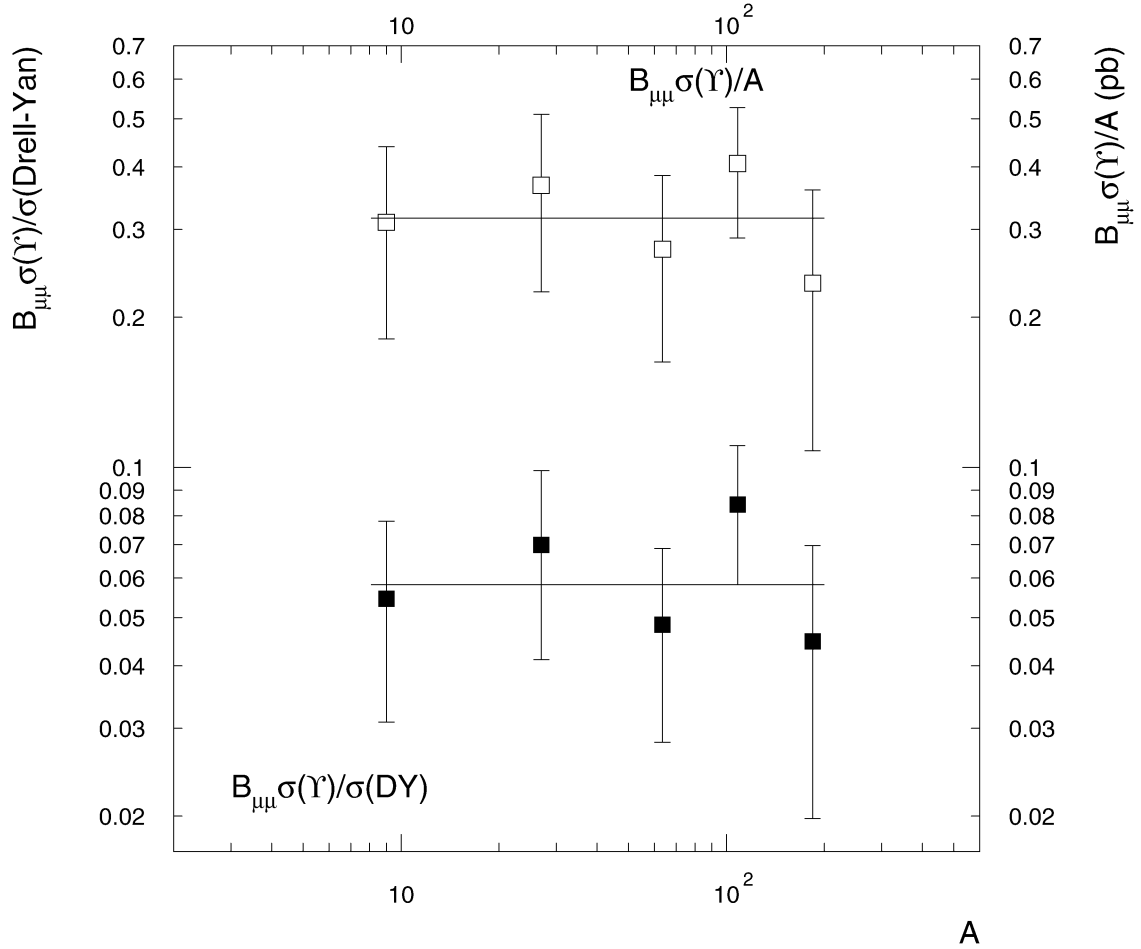
Fig. 4. The ratio $B_{\mu\mu}\sigma\Upsilon / A_{DY}$ (closed squares) and the cross-section per nucleon $B_{\mu\mu}\sigma\Upsilon / A$ (open squares), as a function of A, for the low-intensity data sample.

Finally, we have investigated the A-dependence of the dimuon transverse momentum distributions. In Figs. 6 and 7 we show, for the various systems, the p_T spectra observed in the mass intervals $4.5 < m_{\mu\mu} < 8$ GeV/c^2 and $8.6 < m_{\mu\mu} < 11.6$ GeV/c^2, respectively. In Fig. 6, the Drell–Yan p_T distributions, generated according to Eq. (1) and filtered through the Monte Carlo simulation of the detector, have been fitted to the data with p_0 as a free parameter. In Fig. 7 the spectra have been fitted with a superposition of Drell–Yan and Υ dimuons. For Drell–Yan (dashed lines) the normalizations have been obtained from the fit to the mass distributions of Fig. 1, while the shapes have been extrapolated from the p_T spectra measured in the lower mass range. The Υ events have been generated following Eq. (1), and p_0 has been used as a free parameter in the fits. As a result, we find that for the two mass intervals under study our fits nicely reproduce the observed p_T distributions. In Table 3 we summarize the p_0 values obtained for the various systems, for both Drell–Yan and Υ. The calculated $\langle p_T \rangle$ and $\langle p_T^2 \rangle$ are also shown. To test the stability of our results on the choice of the assumed Drell–Yan p_T distributions, we have performed a similar study, fitting our data to a PYTHIA calculation, performed with the GRV94LO set of parton distribution functions. The value of the intrinsic $\langle k_\perp \rangle$ of partons inside hadrons, used in PYTHIA, has a strong influence on the

Drell–Yan p_T distribution. It has been tuned directly on the data, obtaining values ranging from 0.88 to 0.90 GeV/c. We find that the shape of the PYTHIA p_T distribution still reproduces our data, with a slightly worse χ^2/ndf. The calculated $\langle p_T \rangle$ differ by less than 3% (7% for $\langle p_T^2 \rangle$) from the result obtained using Eq. (1).

According to [35,36], for heavy quarkonia and Drell–Yan production, initial state parton scattering is responsible for the increase of $\langle p_T^2 \rangle$ observed in p–A collisions with respect to pp. Such an increase is approximately linear as a function of L, the mean length of nuclear matter crossed by the incoming parton, and its size is smaller (by a factor 4/9) if the scattering process is initiated by a quark rather than by a gluon. In Ref. [32] it was shown that the transverse momentum distribution of the J/ψ mesons produced in p–A and A–A collisions can be fitted with the function $\langle p_T^2 \rangle = \langle p_T^2 \rangle_{pp} + a_{gN} \cdot L$, with $a_{gN} = 0.077 \pm 0.002$ (GeV/c)^2 fm^{-1}. In Fig. 8 we show the L-dependence of $\langle p_T^2 \rangle$ for Drell–Yan dimuons in the mass region $4.5 < m_{\mu\mu} < 8$ GeV/c^2, where the initial hard parton is a quark rather than a gluon. A linear increase of $\langle p_T^2 \rangle$ with L is visible. By using the same kind of fit, we get $a_{qN} = 0.021 \pm 0.019$ (GeV/c)^2 fm^{-1}, a value significantly lower than $a_g N$ and, within the rather large errors, in agreement with the expected 4/9 factor. For Υ production, where both $q\bar{q}$ and gg initial states contribute [34],
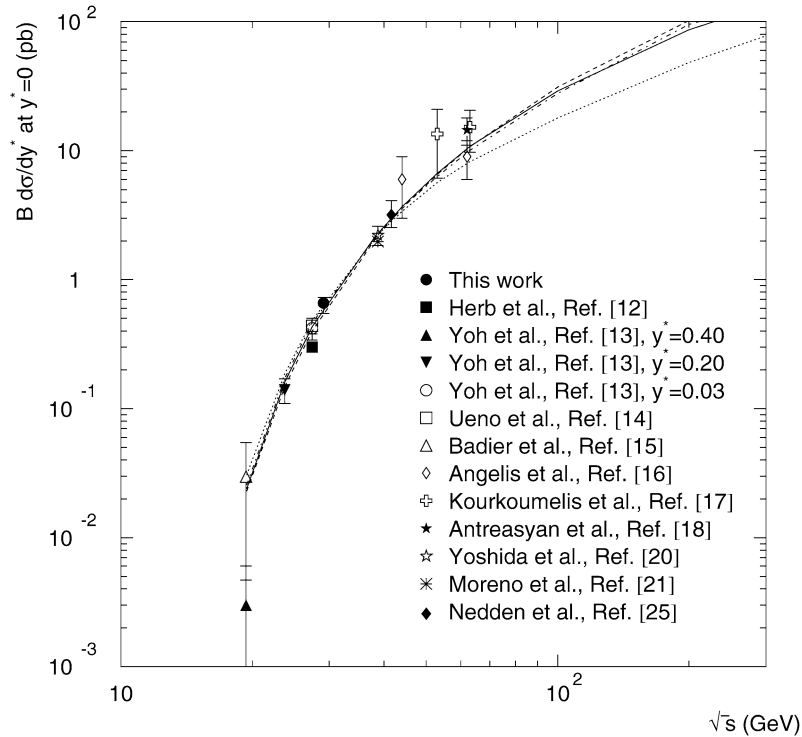
Fig. 5. Υ cross-section at midrapidity as a function of $\sqrt{s}$ The lines represent the results of NLO CEM calculations [33]. The solid, dashed and dot-dashed lines are obtained with the MRST HO PDF set with, respectively, $m_b = \mu = 4.75$ GeV/c^2, $m_b = \mu/2 = 4.5$ GeV/c^2, and $m_b = 2\mu = 5$ GeV/c^2. The dotted line is obtained with the GRV HO PDF set with $m_b = \mu = 4.75$ GeV/c^2. It is assumed that $\mu = \mu_R = \mu_F$, where μ_R is the renormalization scale and μ_F is the factorization scale.
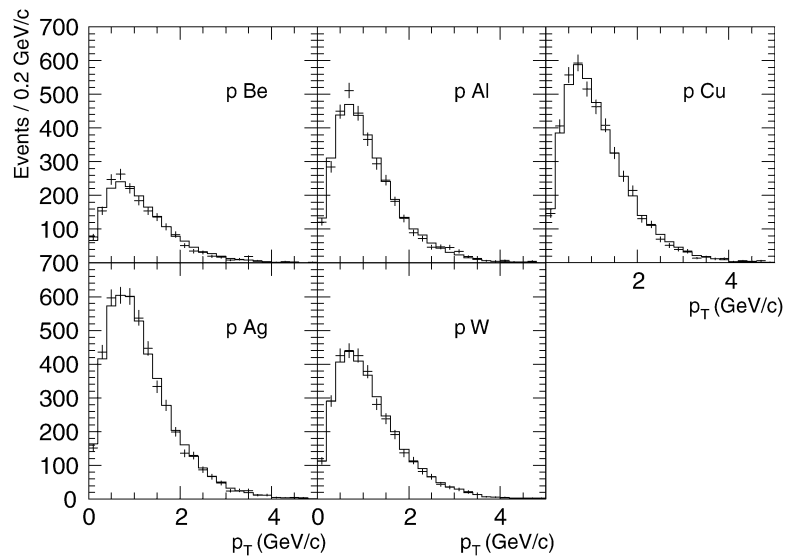

Fig. 6. The measured p–A opposite-sign dimuon p_T spectra in the invariant mass region $4.5 < m_{\mu\mu} < 8.0$ GeV/c^2. The lines represent the best fit to the data obtained with the functional form shown in Eq. (1).

we would expect for the $\langle p_T^2 \rangle$ increase vs. L an intermediate slope between the ones observed for Drell–Yan and J/ψ. Unfortunately, the available statistics (see Fig. 8) does not allow to draw quantitative conclusions. Finally, in Fig. 9 we compare, as a function of $\sqrt{s}$, the measured $\langle p_T \rangle$ (averaged over the various target nuclei) with the results of other experiments. For Drell–Yan, a clear increase of $\langle p_T \rangle$ with $\sqrt{s}$ is observed, while the effect is less important for the Υ.

4. Conclusions

The NA50 experiment measured high-mass ($m_{\mu\mu} > 6$ GeV/c^2) Drell–Yan dimuons and, for the first time, Υ production in p–A collisions at $\sqrt{s} = 29.1$ GeV. By fitting the cross-section results with the usual A^α parameterization, we get $\alpha_{DY} = 0.98 \pm 0.02$ and $\alpha_\Upsilon = 0.98 \pm 0.08$. Within the rather large experimental errors, this result indicates the absence of
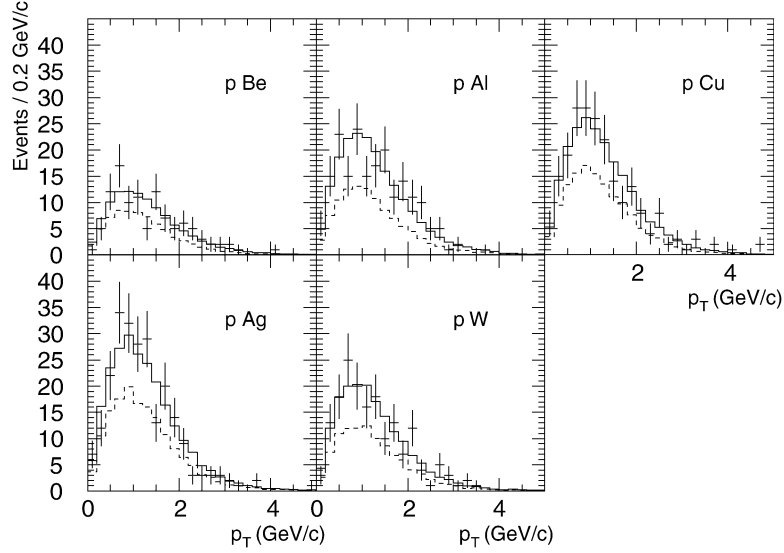
Fig. 7. The measured p–A opposite-sign dimuon p_T spectra in the invariant mass region $8.6 < m_{\mu\mu} < 11.6$ GeV/c^2. The dashed lines represent the contribution of the Drell–Yan process, the solid lines the sum of the Υ and Drell–Yan yields (see text for details).

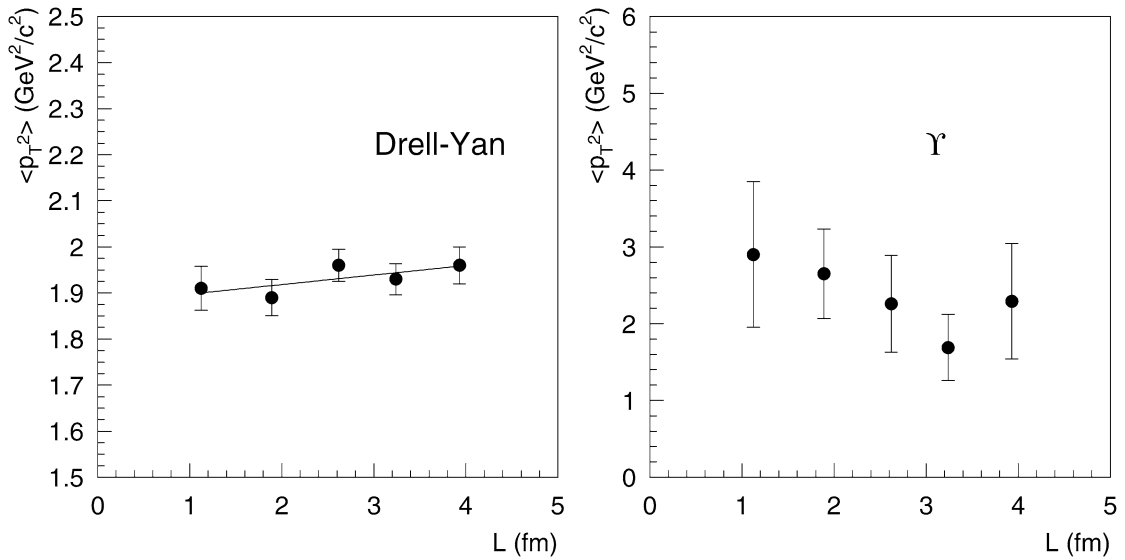Fig. 8. The L-independence of the average transverse momentum squared for Drell–Yan dimuons in the mass range $4.5 < m_{\mu\mu} < 8$ GeV/c^2 (left plot) and for Υ (right plot). For Drell–Yan, the result of a linear fit is also shown.

Table 3
p_0 (see Eq. (1)), $\langle p_T \rangle$ and $\langle p_T^2 \rangle$ for Drell–Yan ($4.5 < m_{\mu\mu} < 8.0$ GeV/c^2) and Υ. The quoted errors for Drell–Yan are purely statistical, while the values for the Υ include a systematical error due to the uncertainty in the extrapolation of the Drell–Yan yield into the Υ region

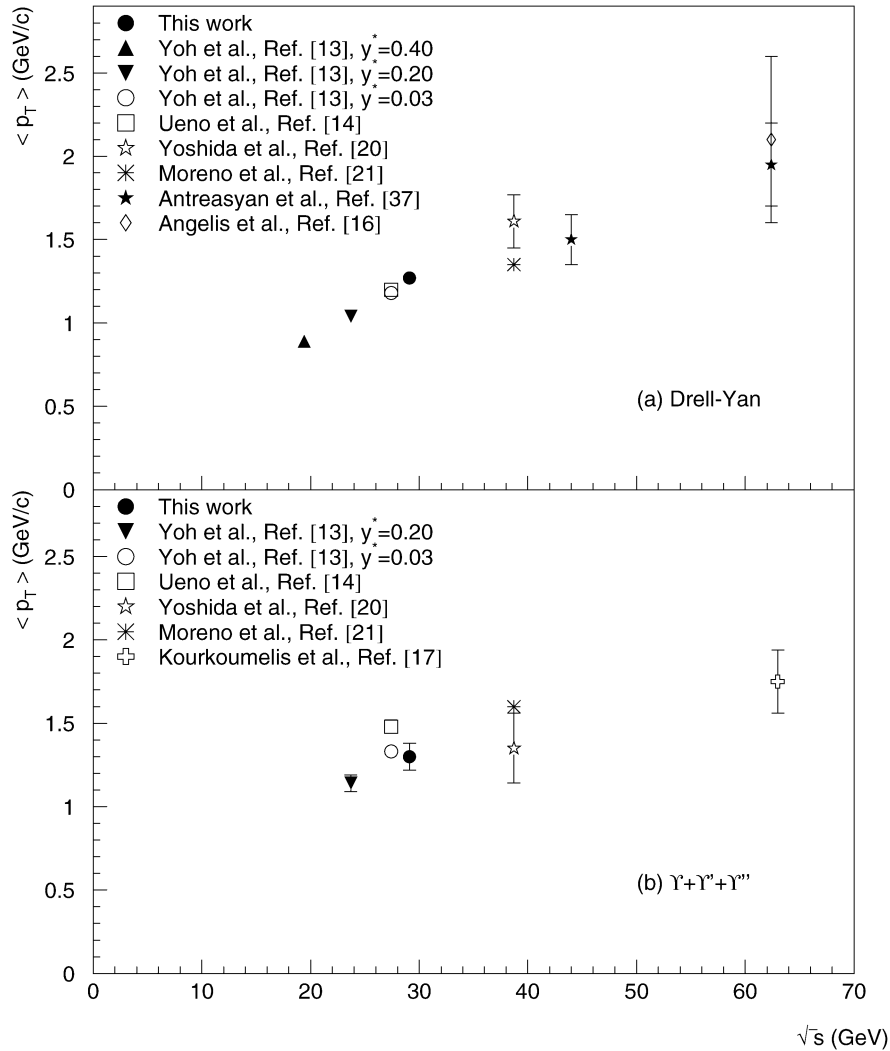|	p_0 (DY) (GeV/c)	p_0 (Υ) (GeV/c)	$\langle p_T \rangle$ (DY) (GeV/c)	$\langle p_T \rangle$ (Υ) (GeV/c)	$\langle p_T^2 \rangle$ (DY) (GeV/c)^2	$\langle p_T^2 \rangle$ (Υ) (GeV/c)^2
p–Be	2.77 ± 0.04	3.4 ± 0.6	1.19 ± 0.03	1.5 ± 0.2	1.91 ± 0.05	2.9 ± 1.0
p–Al	2.75 ± 0.03	3.3 ± 0.4	1.18 ± 0.01	1.4 ± 0.2	1.89 ± 0.04	2.7 ± 0.6
p–Cu	2.80 ± 0.02	3.0 ± 0.4	1.20 ± 0.01	1.3 ± 0.2	1.96 ± 0.04	2.3 ± 0.7
p–Ag	2.78 ± 0.02	2.6 ± 0.3	1.19 ± 0.01	1.1 ± 0.1	1.93 ± 0.03	1.7 ± 0.4
p–W	2.80 ± 0.03	3.0 ± 0.4	1.20 ± 0.01	1.3 ± 0.2	1.96 ± 0.04	2.3 ± 0.7

Fig. 9. The average transverse momentum for Drell–Yan (a) and Υ (b) production as a function of $\sqrt{s}$. For Drell–Yan, the points correspond to $m \sim 0.22 \cdot \sqrt{s}$ (corresponding to $\sqrt{\tau} = m/\sqrt{s} \sim 0.22$).

strong absorption effects for the bottomonium states in nuclear matter. The measured cross-section at mid-rapidity is in good agreement with the results of other experiments in the fixed target energy range and with the available theoretical calculations. The A-dependence of $\langle p_T^2 \rangle$ indicates, for Drell–Yan production, an effect compatible with quark scattering in the initial state.

References

[1] N. Brambilla, et al., hep-ph/0412158.
[2] V. Barger, W.Y. Keung, R.N. Philips, Z. Phys. C 6 (1980) 169;
    V. Barger, W.Y. Keung, R.N. Philips, Phys. Lett. B 91 (1980) 253.
[3] G.T. Bodwin, E. Braaten, G.P. Lepage, Phys. Rev. D 51 (1995) 1125.
[4] V.B. Kopeliovich, A.V. Tarasov, J. Hüfner, Nucl. Phys. A 696 (2001) 669.
[5] F. Arleo, P.B. Gossiaux, T. Gousset, J. Aichelin, Phys. Rev. C 61 (2000) 054906.
[6] R. Vogt, Phys. Rev. C 61 (2000) 035203.
[7] T. Matsui, H. Satz, Phys. Lett. B 178 (1986) 416.
[8] NA50 Collaboration, M.C. Abreu, et al., Phys. Lett. B 477 (2000) 28.
[9] NA50 Collaboration, B. Alessandro, et al., Eur. Phys. J. C 39 (2005) 335.
[10] NA50 Collaboration, B. Alessandro, et al., Phys. Lett. B 553 (2003) 167.
[11] NA50 Collaboration, B. Alessandro, et al., Eur. Phys. J. C 33 (2004) 31.
[12] S.W. Herb, et al., Phys. Rev. Lett. 39 (1977) 252.
[13] J.K. Yoh, et al., Phys. Rev. Lett. 41 (1978) 684.
[14] K. Ueno, et al., Phys. Rev. Lett. 42 (1979) 486.
[15] J. Badier, et al., Phys. Lett. B 86 (1979) 98.
[16] A.L.S. Angelis, et al., Phys. Lett. B 87 (1979) 398.
[17] C. Kourkoumelis, et al., Phys. Lett. B 91 (1980) 481.
[18] D. Antreasyan, et al., Phys. Rev. Lett. 45 (1980) 863.
[19] S. Childress, et al., Phys. Rev. Lett. 55 (1985) 1962.
[20] T. Yoshida, et al., Phys. Rev. D 39 (1989) 3516.
[21] G. Moreno, et al., Phys. Rev. D 43 (1991) 2815.
[22] D.M. Aide, et al., Phys. Rev. Lett. 66 (1991) 2285.
[23] T. Alexopoulos, et al., Phys. Lett. B 374 (1996) 271.
[24] E866 Collaboration, C.N. Brown, et al., Phys. Rev. Lett. 86 (2001) 2529.
[25] HERA-B Collaboration, M. Nedden, et al., hep-ex/0406042.
[26] NA50 Collaboration, M.C. Abreu, et al., Phys. Lett. B 410 (1997) 327.
[27] NA38 Collaboration, M.C. Abreu, et al., Phys. Lett. B 444 (1998) 516.
[28] R. Shahoyan, PhD thesis, Universidade Técnica de Lisboa, 2001.
[29] J.C. Collins, D.E. Soper, Phys. Rev. D 16 (1977) 2219.
[30] M. Clück, E. Reya, A. Vogt, Z. Phys. C 67 (1995) 433.
[31] Particle Data Group, S. Eidelman, et al., Phys. Lett. B 592 (2004) 1.

[32] NA50 Collaboration, N.S. Topilskaya, et al., Nucl. Phys. A 715 (2003) 675c.

[33] R. Vogt, Phys. Rep. 310 (1999) 197;
R. Vogt, Heavy Ion Phys. 18 (2003) 11.

[34] M. Beneke, I.Z. Rothstein, Phys. Rev. D 54 (1996) 2005.

[35] J. Hüfner, Y. Kurihara, H.J. Pirner, Phys. Lett. B 215 (1988) 218.

[36] J.P. Blaizot, J.Y. Ollitrault, Phys. Lett. B 217 (1989) 392.

[37] D. Antreasyan, et al., Phys. Rev. Lett. 47 (1981) 12.